

# Road Tracking, Lane Segmentation and Obstacle Recognition by Mathematical Morphology

Xuan Yu, Serge Beucher and Michel Bilodeau

Ecole des Mines de Paris, Centre de Morphologie Mathématique  
35 rue St-Honore, 77305 Fontainebleau Cedex, FRANCE

Phone :33-1-64-69-47-06, Fax :33-1-64-69-47-07, Email :beucher@cmm.ensm.fr



## Abstract

We present in this paper the work performed at the C.M.M. as part of the European PROMETHEUS project. Our research deals with the road edge detection, lane segmentation and obstacle recognition in a dynamic scene acquired by a monochrome monocular camera. The image processing is based on morphological segmentation tools. The experiments on over a thousand images show that our approach works well on difficult cases such as dense traffic, and roads without land markers.

**Key words:** segmentation, watershed, recognition.

## 1 Introduction

Security improvement to reduce accidents is the major aim of the European PROMETHEUS project for development of intelligent vehicles. Such a vehicle should be able to detect and follow automatically the roads, lanes and obstacles. The research in this area began in the 1970's, and have been considered with increasing interest over the past few years.

The road detection algorithms can be classified in color pixels classification [9], white line recognition [6], and correlation [4]. These methods are based upon the hypothesis that the road edges are visible near the vehicle, which is not verified in the case of dense traffic where the road edges may be hidden by vehicles. Some of them need a road model or white lane markers, this could not be convenient in the case of sharp change of geometrical model, or country road without white land markers.

Various algorithms have been developed for obstacle detection : optical flow fields [5], telemeter approach [1], stereo matching [7].

Our approach is based on monochrome images. For road and lane tracking, no geometrical model is necessary, and the algorithm runs in the case of roads with or without land markers, and in free traffic or dense traffic. Our obstacle detection algorithm consists in extraction of obstacle candidates and verification of obstacle characteristics.

In the following section, mathematical morphology segmentation tools are presented first, then algorithms for road and lane detection and obstacles recognition are described. Finally the results of their application to some image sequences are shown.

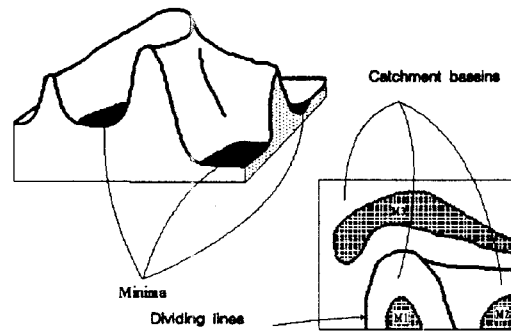


Figure 1: *Topographic surface, minima, catchment basins*

## 2 Segmentation tools

One of the most important tools in mathematical morphology is the watershed transformation. Only essential notions are going to be studied here, see [8] and [2] for more details. An intuitive definition of the watershed is given by considering the graph of image  $f$  as a topographic surface (fig. 1). This surface presents minima, which are connected regions where it is not possible to reach a point at a lower altitude by an always descending path. Suppose that minima are pierced and that the topographic surface is progressively immersed in water. The water will pour through the holes, through the deepest ones at first, and will progressively flood the surface. While flooding, we construct dams at any point where water coming from two different minima may merge. At the end of the flooding, dividing lines appear, called watersheds of the function  $f$ . The different connected components separated by a watershed line are called catchment basins, each of them being associated with a single minimum. The watershed can be a marker oriented segmentation if we impose new minima to  $f$  (figure 2). Doing so, we modify  $f$  while keeping edge information. The watershed on such modified  $f$  will give new catchment basins (and divide lines) related to the imposed minima.

## 3 Road tracking

The road segmentation is done in three steps [3]. The first is the pre-treatment which removes noise on the images. The

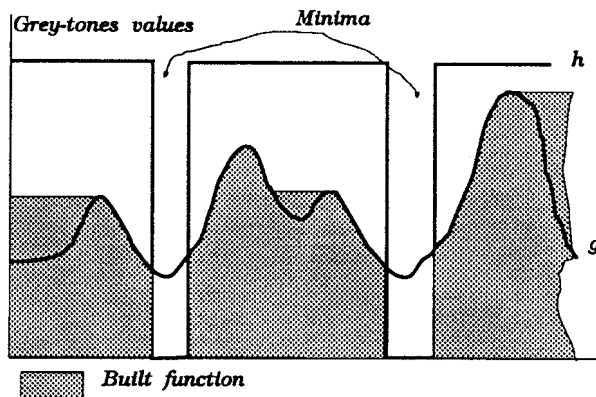


Figure 2: Imposed minima on a function  $g$  and its modification  $h$

second step constructs a mask by means of the watershed of the gradient image. The last step is the watershed controlled by the filtered mask to obtain final road edges.

### 3.1 Pre-treatment

This pre-treatment is performed to remove noise on the images. Special care must be taken to preserve edges. To do so, we have developed a time convolution filter and a time median filter. Both methods are similar; they perform a convolution or a median on a set of sequential images.

Let  $o_n$  be the current image at the time  $n$ . Images  $o_{n-1}, o_{n-2}, \dots, o_{n-m}$  are the  $m$  precedent images. The time convolution filter can be defined as :

$$f_n(i, j) = \sum_{k=0}^m w_k o_{n-k}(i, j)$$

where  $m + 1$  is the number of images,  $w_k$  weights for the convolution and  $f_n$  the result. In practice, this convolution is made on about 5 images. We find experimentally that the weight is not very important, as long as it decreases as the age of the images increases.

Time median filtering can be defined as :

$$m_n(i, j) = \text{med} \left[ \begin{array}{c} o_n(i, j), o_{n-1}(i, j), \dots, \\ o_{n-m}(i, j) \end{array} \right]$$

where "med" stands for the median value of the sequence.

Even if this filtering is done on a time basis, it also filters spatially since all objects in the scene move parallel to the camera. The vertical filtering is more important than the horizontal one because there is more movement in the direction of the camera. The time median preserves more the edges, but it is more time consuming. Practically, we are mainly using the time convolution filter. Figure 8b shows the results of the time convolution filter on the original image (fig. 8a).

### 3.2 Morphological regularized gradient and primitive watershed

A segmentation by watershed without markers is done to extract markers for the final segmentation, see [3] for more

details about this algorithm. The gradient of an image gives a good edge information. Therefore, the watershed transformation is often applied to gradient modulus to locate dividing lines at the edges of objects. But, the watershed on normal gradient is often over-segmented because there are too many minima due to noise (fig. 8c). To reduce the number of minima we are using a regularized morphological gradient defined as follows:

$$g^* = \max_i [TH_i(f \oplus iB - f \ominus iB) \ominus (i-1)B] \quad (1)$$

where  $f$  is the original image,  $g^*$  is the regularized morphological gradient,  $iB$  a disk-shaped structuring element with radius  $i$ ,  $\max$  the maximum between the images,  $\oplus$  the morphological dilation,  $\ominus$  the morphological erosion, and finally  $TH_i$  the top-hat transformation of size  $i$  with the following definition :

$$TH_i(f) = f - ((f \ominus iB) \oplus iB) \quad (2)$$

Figure 8d shows the watershed performed on the regularized gradient of the image of figure 8b.

A binary marker (fig. 8e) is obtained from the previous image by a simple selection of the region located on the foreground of the scene. The marker is smoothed, its holes are filled to give an inner marker (called "inner" because it is inside the road). This marker is complemented and eroded to build an outer marker (fig. 8f).

### 3.3 Final watershed : road edges

The inner and outer markers is then used to modify the gradient image by imposing new minima. Then, the watershed transformation is performed on this modified gradient. The dividing lines of the watershed give the road edges (fig 8g).

## 4 Lanes segmentation

In the previous section, the variation of the contrast between the regions was needed in the segmentation, therefore, the gradient function was used. But it is also possible to apply the watershed to other functions corresponding to other criteria of segmentation. For example, we can use the continuous or broken lines which may separate the traffic lanes. These lines are easily detected by a top-hat transform. The lane markers are then used to control the lane segmentation in a process similar to the road segmentation [3].

## 5 Obstacle recognition

### 5.1 Philosophy

It is very difficult and time consuming to discriminate between all types of obstacles. In fact, it is useless to do so. For example, it is not important to know whether the obstacle is a cow or a horse. What is really essential is to estimate the obstacle position, dimensions, and its projected motion,

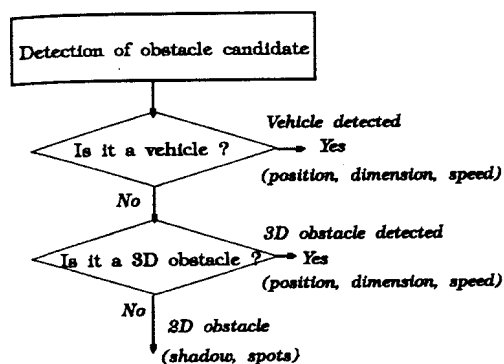


Figure 3: Diagram of obstacle recognition

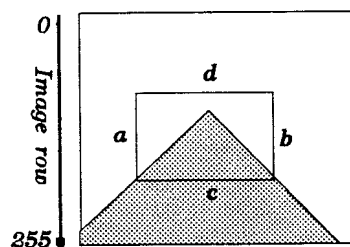


Figure 4: Window of interest

and to determine whether it is really a 3D object or a 2D false obstacle as shadows or spots. Therefore, the possible obstacles are classified in three classes, as shown in figure 3.

## 5.2 Window of interest

In this paper, we only present the module of obstacle candidates detection and vehicle recognition. The 3D module will be performed by a telemeter implemented by another group of PROMETHEUS in France [1]. Both the high resolution from the video vision, and 3D reliability from telemeter are used in such a coupled configuration.

To reduce the recognition processing time, window of interest (WOI) is obtained from the result of road detection described above (fig. 4). One of the results of our road detection scheme is to give the free distance ahead. The lower limit  $c$  of the WOI is just put at this distance. The sides  $a$  and  $b$  are located at the left and right road edge respectively. The upper  $d$  is located at an image row defined by:

$$r_d = \min(r_v, r_h)$$

where  $r_v$  is the image row corresponding to the top of vehicle ahead, situated at position  $c$  with a maximum height,  $r_h$  is the image row of horizon. The window determined in this way is automatically adapted to the road geometry and traffic situation for optimizing recognition processing time. So, the module for road tracking is coupled with the module of obstacle recognition in our system.

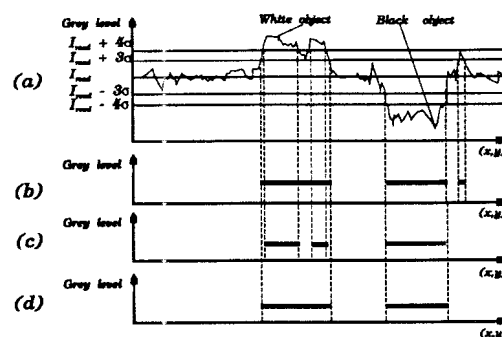


Figure 5: Automatic and adaptive thresholding

## 5.3 Obstacle candidates detection

The main problem in getting fine obstacle outlines is to extract markers identifying potential obstacles.

If we consider the image intensity, the objects on the road are characterized only by the difference of luminances between them and the road (fig. 5a). The observation of a large number of images acquired under different conditions, have showed that the luminances for painted components of the vehicle may be various and sometimes the same as the road luminance, but the head or tail of vehicle is always much darker than the road. We therefore extract the binary markers by thresholding the original image, which is a simple and fast operation. But the choice of threshold should be automatic and adaptive to the images acquired in different conditions, and the binary markers resulting from threshold should verify the following conditions:

- only one connected component for one object
- the markers should be large enough to cover the objects themselves, so that the region contours generated by the watershed are located at the outer outlines of the objects.

These conditions are verified by analyzing the masked histogram in a window placed just ahead of the vehicle (fig. 6a), which can be determined, similar to the WOI above, by the result of road segmentation. This zone contains mostly the road pixels without obstacles. The curve of the histogram is multi-modal with the road as the dominant mode (fig. 6b). The variance for road mode  $\sigma$  is calculated by searching around the maximum peak or by another technique: the random spots are always of limited dimension, for example, less than several meters. If we accumulate the masked histograms for several images of the sequence, the road corresponding mode exists in each image but not for random spots. In this way, the random spot modes are attenuated, and the variance calculated on the whole masked histogram can be used directly as road luminance variance  $\sigma$ .

Once  $\sigma$  is obtained, a threshold  $S_{low}$  is determined by  $I_{road} \pm 3\sigma$  (fig. 5a). Outside this band, the number of road pixels is small. This technique means that all the pixels in the band  $I_{road} \pm 3\sigma$  belong to the road, and the others belong to

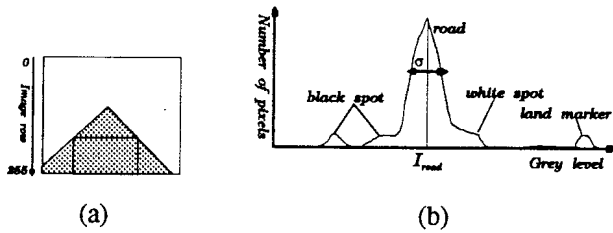


Figure 6: Window for masked histogram

possible obstacle candidates. All the binary markers obtained by this threshold are large and they are connected components (fig. 5b, fig. 8h). On these figures, some road pixels are outside the band  $I_{road} \pm 3\sigma$ , generating false markers. We propose here a fast method to reduce the number of false markers. The difference between obstacle intensity and road intensity should be more important than road intensity variation (otherwise, the signal/noise ratio is too low to extract a useful pattern.). Another threshold  $S_{high}$  placed farther than  $I_{road} \pm 3\sigma$  (for example,  $4\sigma$ ) will eliminate false candidate markers, but a real marker may be subdivided into several separated ones (fig. 5c, fig. 8i). The binary morphological reconstruction of the figure 5c in 5b (or fig. 8i in fig. 8h) gives the final marker (fig. 5d, fig. 8j), where the false marker does not occur and each real marker is a connected component. The binary reconstruction is a very fast transformation for a morphological machine. As for the first threshold  $S_{low}$ , the second threshold  $S_{high}$  can also be determined automatically with respect to  $S_{low}$  by:

$$S_{high} = I_{road} \pm N\sigma$$

where

$$N\sigma/3\sigma = N/3 = R_{min}$$

or

$$N = 3R_{min}$$

where  $R_{min}$  is the minimum ratio of signal/noise (for example 1.5), above which all the signals are detected.  $R_{min}$  remains the only parameter to be determined. The concept of a minimum  $S/N$  ratio is familiar to electrical engineers, and it can then be easily determined by experience in other areas. In our case, we recommend to use a low  $R_{min}$  because we prefer false alarm to omitted obstacles (there are other criteria to be used to reject false alarms, that we will present in the following section).

In fact, these binary markers are often near the object outlines. One can take them directly as outlines of candidates obstacles. If one hopes to get more accurate outlines, the application of watershed with these markers gives satisfactory results (fig. 8k).

#### 5.4 Vehicle characteristics checking

Among the obstacle candidates, some of them are vehicles, which can be extracted by some criteria. We propose here a

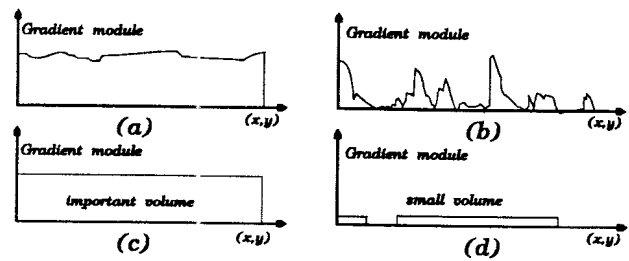


Figure 7: Directional gradient, its linear opening and its effects on the volume

criterion driven from the following observation: the head or tail of a vehicle is always composed of some horizontal line segments.

To apply this criterion, the morphological directional gradient in the vertical direction is applied to the original image, giving the module of gradient in that direction. The module values are large on the horizontal lines situated at the edges of man-made objects (fig. 7a), but not for the horizontal lines situated elsewhere (fig. 7b). Then, a morphological directional opening in the horizontal direction allows to eliminate noise gradient module (fig. 7d), without attenuating significantly the gradient module of the horizontal lines (fig. 7c). Finally, a measurement of the volume  $v$  normalized by the area on the result image gives a scalar value. This measurement is a good discriminator between the vehicles and the irrelevant objects. From the results on several image sequences, the value of  $v$  is always superior to 15 for a vehicle, and inferior to 5 for other obstacles as shadows, spots, etc. Thus the decision of classification can be made by an arbitrary threshold in this interval. The figure 8l shows the vehicles finally recognized, by line segments to indicate their positions and dimensions. The speeds of the vehicles as obstacles can be calculated by comparing their positions at different times.

## 6 Experiments on image sequences

We have tested our algorithm on a large number of image sequences, and these results are presented on figure 9. Each sequence is composed of 90 images with an time interval between two successive images equal to 200 ms. The first sequence is a secondary road scene (fig. 9abc). Although there is no land marker to limit the road in this case, the road edges are correctly detected. The second sequence shows a dense traffic situation (fig. 9def), where only the right road edge is visible. The program indicates, as desired, the obstacle free distance ahead of the intelligent vehicle. The third sequence shows a road with the shadow of a bridge (fig. 9ghi). The free distance ahead is reduced because of the shadow, and we need a 3D module to reject the shadow as 2D object. The fourth sequence shows the vehicle detection (fig. 9jkl); with this sequence, we can notice that the range of detection is good and the outlines of detected vehicle are accurate.

## 7 Conclusion

We have developed algorithms for road, lane, and obstacle detection in real traffic situations with some difficulties such as dense traffic, road without land markers, and poor quality of images. The experiments on typical image sequences have given satisfactory results. We are now working on the hardware implementation of algorithms for PROLAB2, a European intelligent vehicle demonstrator designed, in the frame of the PROMETHEUS project, by French laboratories and cars manufacturers.

## Acknowledgments

This research has been supported and granted by European Community fundings for the PROMETHEUS project. Technical support (especially, the images sequences) has been provided by RENAULT and PSA (PEUGEOT/CITROEN group).

## References

- [1] ALIZON J., GALLICE J., TRASSOUDAIN L. and TREUILLET S., "Multi-sensory Data Fusion for Obstacles detection and Tracking on Motorway", Proc. of the Workshop on Vision, Sophia Antipolis, France, April 19-20, 1990.
- [2] BEUCHER S., "Segmentation Tools in Mathematical Morphology", SPIE, Application of Digital Image Processing XIII, San Diego, California, July 1990.
- [3] BEUCHER S., YU X., BILODEAU M., "Road Segmentation by Watershed Algorithm", Proceeding of the Workshop in Vision held in Sophia Antipolis France on April 19-20 1990.
- [4] DICKMANS E.D., and GRAFE V., "Dynamic Monocular Machine Vision", Machine Vision and Applications, 1988, pp223-240.
- [5] ENKELMANN W., "Obstacle detection by Evaluation of Optical Flow Fields", Proc. of the Workshop on Vision, Sophia Antipolis, France, April 19-20, 1990.
- [6] ISHIKAWA S., KUWAMOTO H., and OZAWA S., "Visual Navigation of Autonomous Vehicle Using Line recognition", IEEE Transaction on Pattern Analysis and Machine Intelligence, VOL.10, No.5, Sept. 1988.
- [7] MEYGRET A. and THONNAT M., "Objects Detection in Road Scenes Using Stereo Data", Proc. of the Workshop on Vision, Sophia Antipolis, France, April 19-20, 1990.
- [8] SERRA J., "Image Analysis and Mathematical Morphology", volume 1, Academic press, 1982.
- [9] THORPE C., HEBERT M.H., KANADE T., SHAFER S.A., "Vision and Navigation for the Carnegie-Mellon Navlab", IEEE Transaction on Pattern Analysis and Machine Intelligence, VOL.10, No.3, 1988.

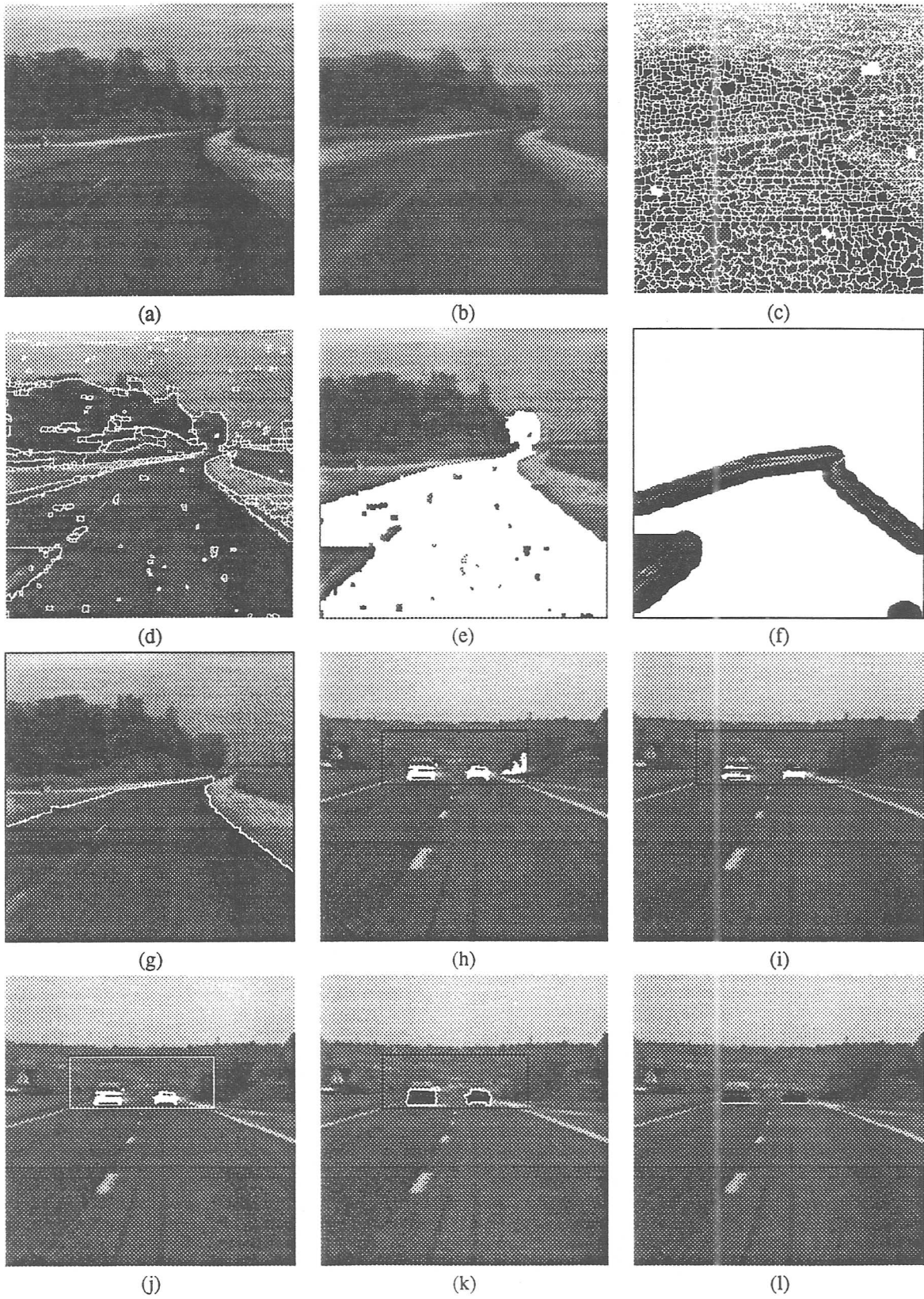
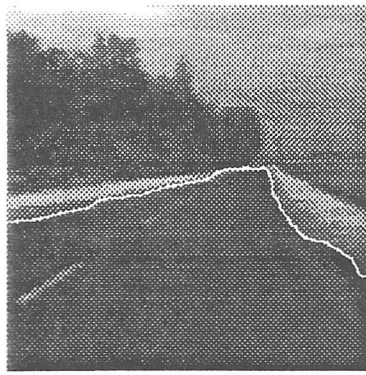


Figure 8: *The various steps of road segmentation and obstacle detection*

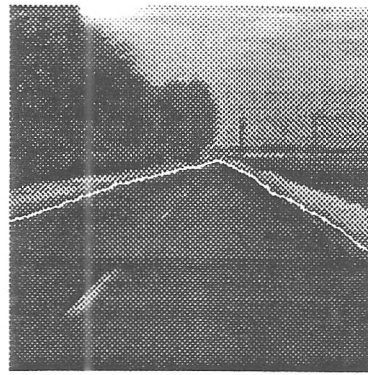




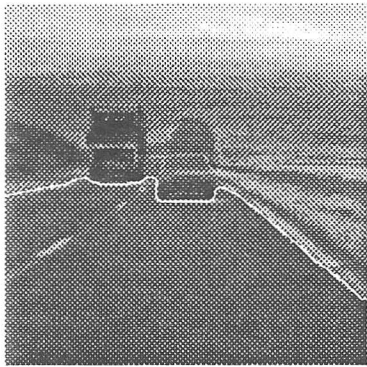
(a)



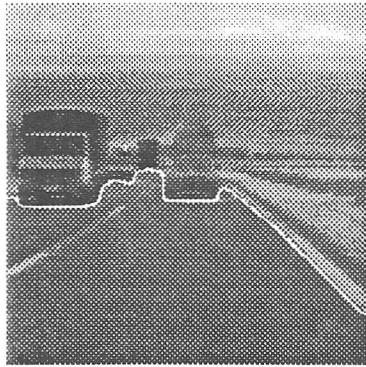
(b)



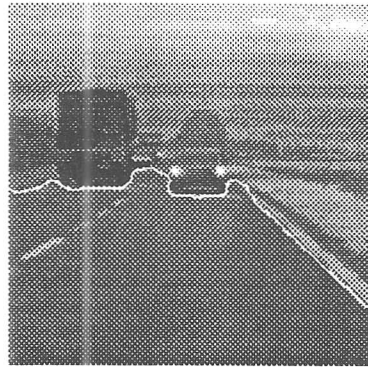
(c)



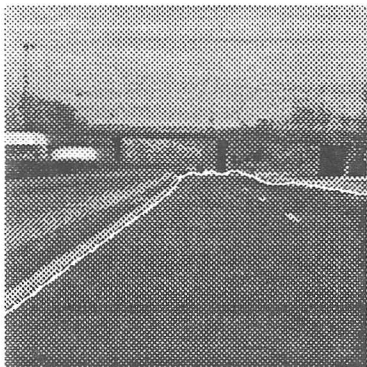
(d)



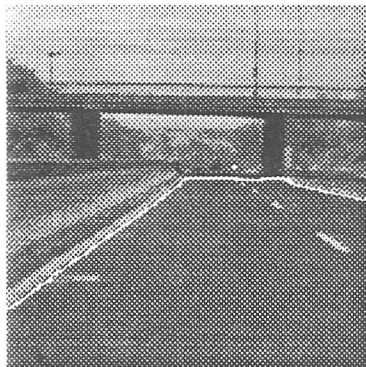
(e)



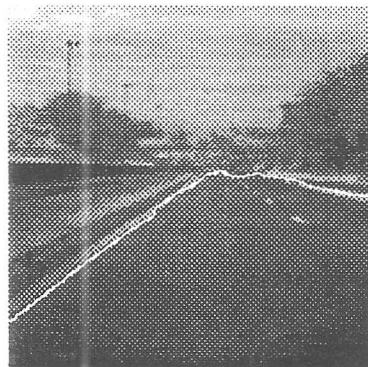
(f)



(g)



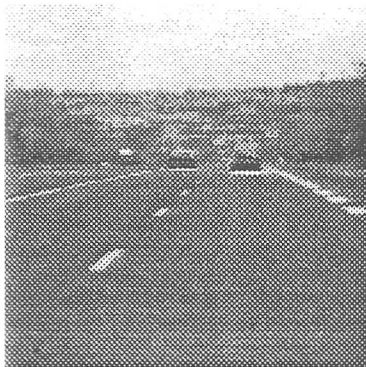
(h)



(i)



(j)



(k)



(l)

Figure 9: Results on image sequences